A Letters Journal Exploring
the Frontiers of Physics

OFFPRINT

Coaction of strain and polarization effects on tuning the photoinduced resistance changes in $La_{0.9}Sr_{0.1}MnO_3$ films

E. J. Guo, J. Gao and H. B. Lu

EPL, **95** (2011) 47006

A Letters Journal Exploring the Frontiers of Physics

August 2011

EPL, **95** (2011) 47006
doi: 10.1209/0295-5075/95/47006

www.epljournal.org

Coaction of strain and polarization effects on tuning the photoinduced resistance changes in $La_{0.9}Sr_{0.1}MnO_3$ films

E. J. Guo[1,2], J. Gao[1(a)] and H. B. Lu[2]

[1] *Department of Physics, The University of Hong Kong - Pokfulam Road, Hong Kong*
[2] *Beijing National Laboratory for Condensed Matter Physics, Institute of Physics, Chinese Academy of Sciences Beijing 100190, PRC*

received 30 March 2011; accepted in final form 27 June 2011
published online 26 July 2011

PACS 72.40.+w – Photoconduction and photovoltaic effects
PACS 71.38.-k – Polarons and electron-phonon interactions
PACS 77.22.Ej – Polarization and depolarization

Abstract – We had epitaxially grown $La_{0.9}Sr_{0.1}MnO_3$ (LSMO) thin films on ferroelectric 0.67Pb($Mg_{1/3}Nb_{2/3}$)O_3-0.33$PbTiO_3$ (PMN-PT) single-crystal substrates. The electric-field controls of transport and photoinduced resistance (PR) changes were observed in LSMO films. The variations of PR under different electric fields applied to the LSMO/PMN-PT structure were quite different when PMN-PT was in positively and negatively polarized states, which can be attributed to the coaction of both electric-field–induced lattice strain effect and ferroelectric polarization effect. These results provide us another route to see the nature of modulating the properties of manganite films by external electric fields.

In the past decades, great efforts had been devoted to the perovskite-type manganites due to their variety of interesting properties and potential device applications. The observation of colossal magnetoresistance (CMR) in the doped manganites has greatly stimulated the researches on this kind of strongly correlated electron systems [1]. It was found that the physical properties of the doped manganites were dramatically affected by external fields, such as electric and magnetic fields [2,3], pressures [4], and light [5–9], which could change the strength of the double-exchange (DE) interaction and Jahn-Teller (J-T) electron-lattice coupling in the manganites. Among them, the electric-field–induced polarization effect and converse piezoelectric effect on manganites were extensively studied by the combination of manganite films and ferroelectric single crystals. Thiele *et al.* [10] and Zheng *et al.* [11] found that the ferroelectric poling induced a lattice strain in the substrates via the converse piezoelectric effect, dominating over the field effect, subsequently resulting in the change of the strain state and resistance of the manganite films. However, some works pointed out that the field-induced polarization effect should also be considered besides the lattice strain effect. Hong *et al.* [12] found that the polarization field of a ferroelectric oxide, $Pb(Zr,Ti)O_3$, can electrostatically modulate the metallicity of ultrathin manganite $La_{1-x}Sr_xMnO_3$ (LSMO) films by depleting holes in the films. The experimental measurements in $La_{0.7}Ca_{0.3}MnO_3$/(1-x)Pb($Mg_{1/3}Nb_{2/3}$)O_3-$x$$PbTiO_3$ structures revealed that the coaction of two factors, electric-field–induced strain and polarization effect, was responsible for tuning the properties of manganites [13]. All these features demonstrate that the detailed electric-field–induced effects on the electric and magnetic properties of manganite films are far from being fully understood and still need further investigation.

On the other hand, among all the photoinduced effects in manganites, the photoinduced demagnetization was intensively studied. Laser-excitation–induced conductance changes and demagnetization will strongly affect the transport and magnetic properties of doped manganites by modulating the interactions among spin, charge, and lattice and also the relaxation processes of the nonequilibrium state of manganites [5–9]. Therefore, the investigation of the electric-field–mediated properties of manganite films through optical measurements has rarely been reported. In this letter, we studied the electric-field–induced ferroelectric polarization and strain effects on the photoinduced demagnetization of LSMO films. Tuning the photoinduced resistance changes of the

(a) E-mail: jugao@hku.hk

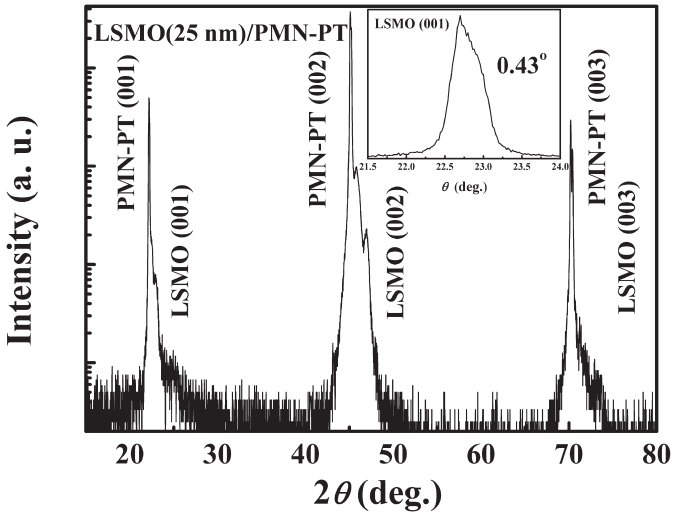

Fig. 1: X-ray diffraction (XRD) spectra of single-phase LSMO films grown on PMN-PT. The inset shows the rocking curve of the (002) reflection of LSMO.

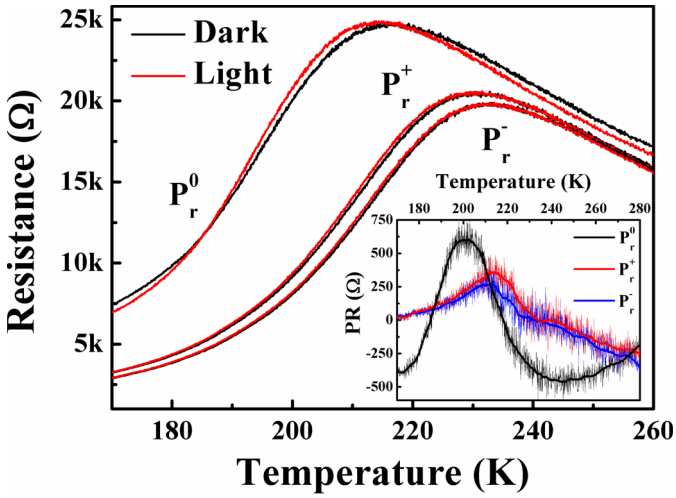

Fig. 2: (Color online) The temperature dependence of resistance for the LSMO film kept in the dark and under the irradiation of 532 nm laser when PMN-PT was in $P_{\rm r}^0$, $P_{\rm r}^+$, and $P_{\rm r}^-$ states, respectively. The inset shows the PR changes of the LSMO film with temperature when PMN-PT was in $P_{\rm r}^0$, $P_{\rm r}^+$, and $P_{\rm r}^-$ states, respectively.

films were observed by applying different electric fields in the $La_{0.9}Sr_{0.1}MnO_3/0.67Pb(Mg_{1/3}Nb_{2/3})O_3$-$0.33PbTiO_3$ (LSMO/PMN-PT) structure. These results provided us another route to see the nature of electric-field–induced strain and polarization effects on manganites.

Recently, many reports focused on the composition of the manganite films (pseudocubic lattice parameter $c_{\rm films} \sim 3.88$ Å) with ferroelectric PMN-PT single-crystal substrates (pseudocubic unit cell $c_{\rm PMN\text{-}PT} \sim 4.02$ Å) due to their lattice mismatch ($\sim 3.48\%$), large remnant ferroelectric polarization ($P_{\rm r} \sim 22.9\,\mu{\rm C/cm}^2$), and low coercive field (~ 2.8 kV/cm) [10,11]. In our experiment, the LSMO film with thickness of ~ 25 nm was fabricated by pulsed-laser deposition (PLD) using a KrF excimer laser with a wavelength of 248 nm, frequency of 2 Hz, and energy of single pulse ~ 300 mJ [14]. The substrates were (001)-oriented PMN-PT single-crystal wafers with thickness of 0.5 mm. The temperature of the substrates was kept at 700 °C and the oxygen pressure was maintained at 0.2 mbar throughout the deposition. After the deposition, the LSMO films were *in situ* annealed in pure oxygen of ~ 1 atm for 30 minutes. The as-grown LSMO film was in an initial tensile strain due to the lattice mismatch between the film and substrate. X-ray diffraction (XRD) θ-2θ scanning was carried out, as shown in fig. 1. Besides the reflection of the substrate and the $(00l)$ diffraction reflection of the LSMO film, no other reflections from the impurity phases or randomly oriented gains could be observed. We also measured the rocking curve of the (002) reflection of LSMO (shown in the inset of fig. 1). It presents a very small value ($\sim 0.43°$) of full width at half maximum, implying a highly epitaxial growth and good crystallization of the LSMO film.

In order to obtain good contacts for electric measurements, four silver contact pads were prepared on the LSMO films by thermal evaporation. The resistance of the films was measured using the standard four-probe method in a closed-cycle cryostat. The schematic for the LSMO/PMN-PT structure and the measuring circuit are shown in the inset (b) of fig. 3. A 20 MΩ resistance was connected in series with the LSMO/PMN-PT structure in order to avoid dielectric breakdown. We applied a DC poling field E of ± 10 kV/cm across the LSMO/PMN-PT structure by an external high-voltage generator for positively (referred to as $P_{\rm r}^+$) or negatively (referred to as $P_{\rm r}^-$) polarization, respectively (*i.e.*, here, we defined that the electric dipole moment in the PMN-PT point toward the film is the positive direction.). After poling for about 30 minutes, the electric field was turned off and the PMN-PT was in the polarized states. A semiconductor laser with wavelength of 532 nm and power density of 3 mW/cm^2 served as a light source.

Figure 2 shows the temperature dependence of resistance for the LSMO film with and without light irradiation when the PMN-PT substrate was in the unpolarized (referred to as $P_{\rm r}^0$), $P_{\rm r}^+$, and $P_{\rm r}^-$ states, respectively. We can find that, no matter what polarized states of PMN-PT, the resistance of the LSMO film increases with decreasing temperature and undergoes a paramagnetic insulating (PMI) state to ferromagnetic metallic (FMM) state transition. The transition temperatures $T_{\rm c}$ are 215 K, 230 K, and 233 K for the LSMO film when PMN-PT is in $P_{\rm r}^0$, $P_{\rm r}^+$, and $P_{\rm r}^-$ states, respectively. As seen in fig. 2, the resistance of LSMO decreases in a wide range of values after it has been positively polarized and $T_{\rm c}$ shifts upwards by ~ 15 K. It is widely accepted that the ferroelectric-poling–induced lattice strain effect plays an important role on it [10,11]. Through the Poisson effect, the increase of

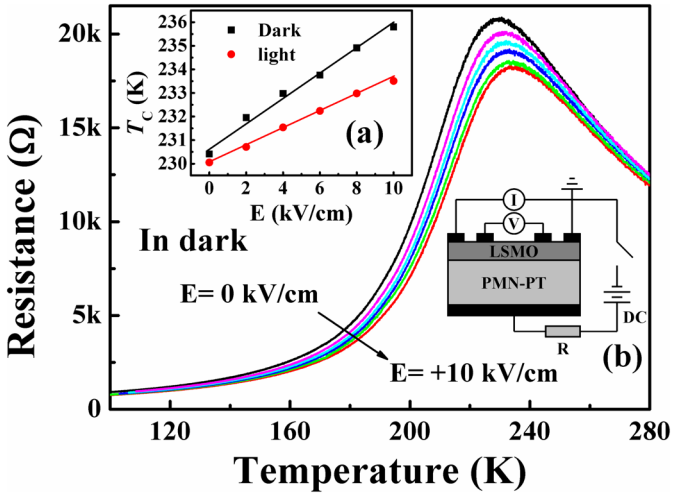

Fig. 3: (Color online) The temperature dependence of resistance for the LSMO film by applying an electric field E from 0 to 10 kV/cm on the LSMO/PMN-PT structure when PMN-PT was in P_r^+ state and measured kept in the dark. The inset (a) shows T_c *vs.* E when LSMO is kept in the dark and under the irradiation of 532 nm laser, respectively. The inset (b) presents the schematic diagram of the LSMO/PMN-PT structure and the measurement circuit.

the lattice parameter c of PMN-PT after poling leads to a decrease in the in-plane tensile strain on the LSMO film, thus resulting in a decrease of the J-T electron-lattice interaction and an enhancement of the DE interaction, which leads to an increase in the hopping of charge carriers. This also results in a decrease in the resistance of the LSMO film and an enhancement of T_c. Besides, many works discussed that the field effect in such structure is negligible since the electronic screening length in the manganite films is rather small, which cannot be compared with the film thickness [11]. In order to clarify this problem, we further measured the resistance of the LSMO film when PMN-PT was in P_r^- states. The same variation trends were observed. However, it should be noted that the magnitude of the decrease in resistance of the film and the increase in T_c (~ 18 K) for P_r^- states is larger than that for P_r^+ states.

The temperature dependence of resistance was also measured under the irradiation of light when PMN-PT is in different polarized states. The photoinduced resistance changes ($\mathrm{PR} = R_{\mathrm{light}} - R_{\mathrm{dark}}$) were present in the inset of fig. 2. All the PRs had negative values when LSMO was in the PMI state, and turned to positive values when LSMO transited to FMM states. The same result was found in ref. [5] and [6]. In the PMI state, the injection of photoexcited carriers and the enhancement in hopping of anti−J-T polarons will lead to a decrease of resistance. Moreover, in the FMM state, the photoinduced demagnetization effect will play a dominant role. Incident light will stimulate spin-down e_g electrons, which are expected to destroy the electron-lattice coupling between spin-up e_g and t_{2g} electrons in Mn^{3+} ions. The PMI/FMM phase balance in LSMO will be changed, favoring the PMI state and suppressing the neighboring spin correlation. The magnetization of LSMO will be greatly influenced by the injection of photoinduced carriers. At the same time, the injection of e_g carriers will weaken the DE, leading to the increase of the LSMO resistance. Therefore, the above results were understandable. Here, note that the PRs of the LSMO film measured in P_r^+ and P_r^- states have little difference. We will further discuss it in the following section.

To study the ferroelectric-poling–induced effects on the transport and photoinduced demagnetization in the LSMO film, we measured the temperature dependence of resistance by applying the electric field E to the LSMO/PMN-PT structure when PMN-PT is in the P_r^+ state. As shown in fig. 3, the resistances of the LSMO film systematically decrease with increasing E from 0 to +10 kV/cm. The relative changes of resistance under 0 and +10 kV/cm are 4.3%, 6.5%, 13.4%, 26.7%, and 24.1% at 280, 250, 230, 210, and 180 K, respectively. We found that the T_c measured under different electric fields increases linearly with increasing E. At the same time, we measured the resistance of the LSMO film under the irradiation of light and got a similar variation as measured kept in the dark except that T_c shifts to a little lower temperature (shown in the inset (a) of fig. 3).

Figure 4(a) shows the temperature dependence of PR under different electric fields E when PMN-PT was in the P_r^+ state. It was found that the PR was strongly modulated by positive electric field E. As shown in fig. 4(b), when E increases from 0 to +10 kV/cm, the maximum PR of the LSMO film increases from 380 to 1150 Ω measured at 215 K. Most of the previous works thought that tuning the transport of doped manganite films was attributed to the ferroelectric-poling–induced strain effect. In order to confirm this possibility, we *in situ* measured the XRD patterns towards the pseudocubic (002) reflection of LSMO films under different E. As shown in the inset of fig. 5, it was found that LSMO pseudocubic (002) reflection shifts toward the lower 2θ value with increasing E from 0 to +10 kV/cm, which indicates that the c-axis lattice parameter was elongated by the tensile strain due to the converse piezoelectric effect. The calculated lattice constant c of LSMO increases from 3.849 to 3.855 Å when E increases from 0 to +10 kV/cm, which leads to the relaxation of the in-plane tensile strain of the film. It is generally believed that the reduction of tensile strain in LSMO will influence the J-T distortion in MnO_6 octahedral structure and then further weaken the electron-lattice coupling.

We also measured the temperature dependence of PR when PMN-PT was in the P_r^- state, as shown in fig. 4(c). However, this time, the PR measured under negative electric fields E kept almost the same values ~ 1300 Ω at 215 K and exhibited nearly no modulation with electric fields (shown in fig. 4(d)). After PMN-PT has been

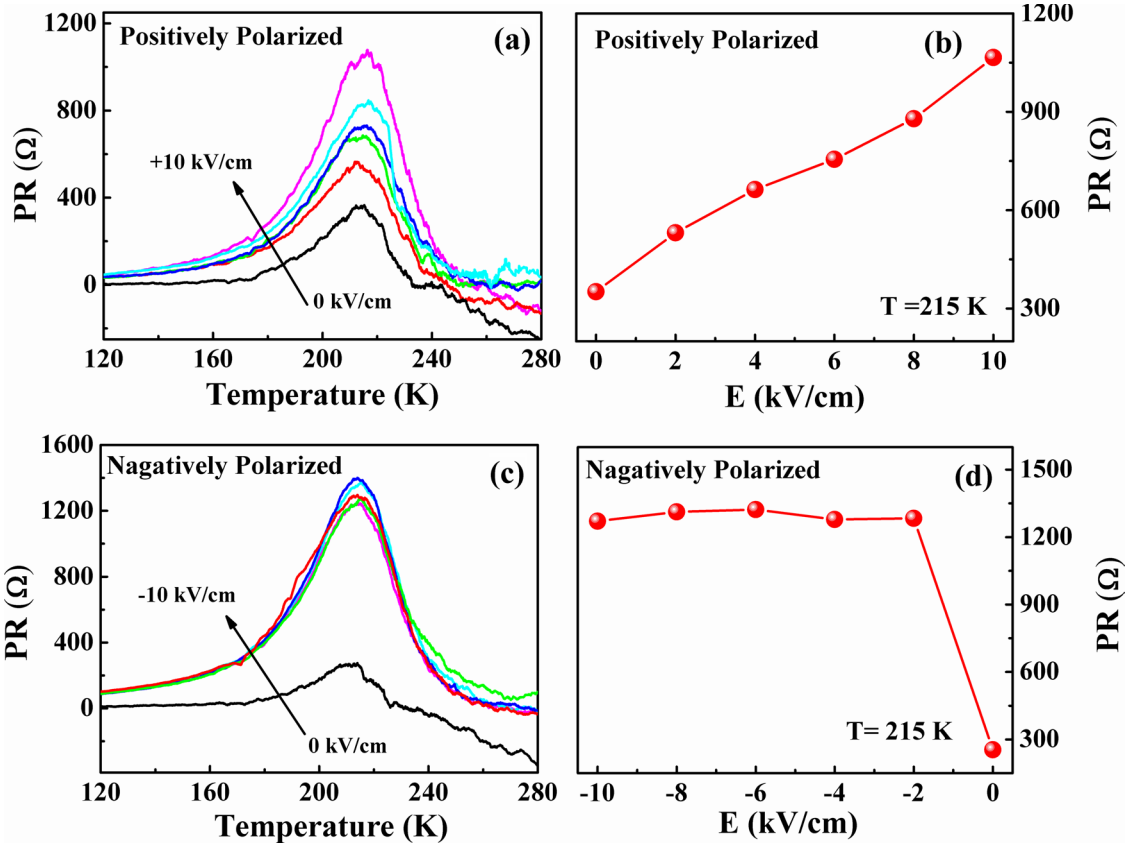

Fig. 4: (Color online) The temperature dependence of photoinduced resistance (PR, where $\mathrm{PR} = R_{\mathrm{light}} - R_{\mathrm{dark}}$) changes for the LSMO film by applying different electric fields to the LSMO/PMN-PT structure when PMN-PT is in (a) P_{r}^{+} and (c) P_{r}^{-} states, respectively. The field dependence of PR for the LSMO film measured at 215 K when PMN-PT is in (b) P_{r}^{+} and (d) P_{r}^{-} states, respectively.

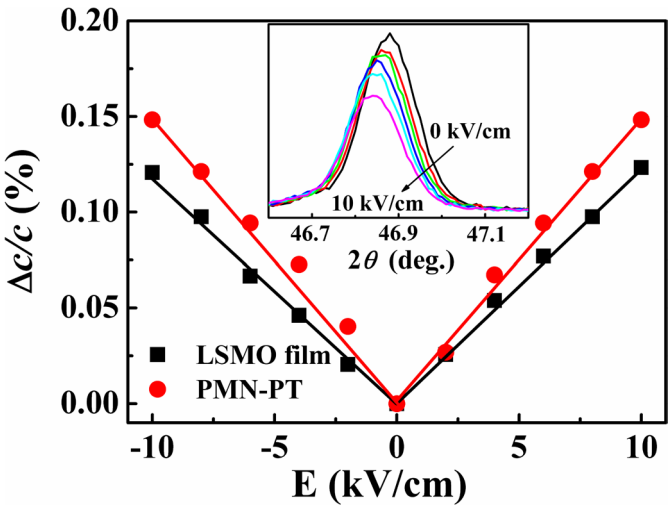

Fig. 5: (Color online) The relative changes in the pseudocubic lattice constants $\Delta c/c$ of the LSMO film and the PMN-PT substrate as a function of electric field E from $-10\,\mathrm{kV/cm}$ to $+10\,\mathrm{kV/cm}$. The inset shows the *in situ* XRD patterns in the vicinity of pseudocubic (002) reflection for the LSMO film under different electric fields.

positively or negatively polarized, the as-grown tensile strain will be little decreased. Then, the positive increase or negative decrease of E at PMN-PT makes it possible to further release the tensile strain of the LSMO film. Figure 5 presents linearly relative changes of the out-of-plane lattice constants $\Delta c/c$ of the LSMO film and the PMN-PT substrate under E from +10 to 0 kV/cm and from 0 to $-10\,\mathrm{kV/cm}$, respectively. We can find that the $\Delta c/c$ of the LSMO film and the PMN-PT substrate had equal values of 0.12% and 0.148%, respectively, whenever E is +10 and $-10\,\mathrm{kV/cm}$. On the other hand, the calculated in-plane tensile strain, $\Delta\varepsilon_{xx}$, of the LSMO film decreases the same value by 0.076% under $E = \pm 10\,\mathrm{kV/cm}$ using the assumed approximate volume-preserving distortion and the expression $\Delta\varepsilon_{zz} = -2v/(1-v)\Delta\varepsilon_{xx}$ (where $v = 0.5$ is the Poisson ratio) [15]. Thus, if only the strain effect is considered, it is hard to understand the differences of PR and T_{c} measured under the same lattice strains which are induced by the same absolute positive and negative electric fields when PMN-PT is in P_{r}^{+} and P_{r}^{-} states, respectively. Therefore, we think the phenomenon observed in our experiment is the result of the coaction of both the electric-field–induced ferroelectric polarization effect and the lattice strain effect. As we all know, LSMO is a p-type material whose majority carriers are holes.

When PMN-PT is polarized, the electric dipole moments in PMN-PT point upward (or downward) to the LSMO film when it is in P_r^+ (or P_r^-) states. Thus, the positive polarization of PMN-PT will lead to the accumulation of electrons and the holes at the interface will be the depleted partially, resulting in a certain increase of the film resistance in the P_r^+ state. However, the total resistance will still decrease because the strain effect plays a major role. At the same time, photoinduced extra carriers in LSMO, which suppress the neighboring spin correlation, may have a high percentage due to the depletion of holes, thus, PR can be tuned greatly by E. On the contrary, the negative polarization will lead to an accumulation of holes, resulting in the further decrease of resistance. As a result of the accumulation of holes, the modulation of PR by E is unobvious. Therefore, the differences of PR, $\Delta R(=[R(P_r^+) - R(P_r^-)])$, and T_c measured under PMN-PT are in P_r^+ and P_r^- states and can be attributed to the field polarization effect.

To gain the insight into the ferroelectric polarization effect on the manganite films, the above measurements had been also carried out on the LCMO films with thickness of $\sim$40 nm grown on the PMN-PT substrate [15]. We observed that the magnitude of PR was modulated by the electric-field, which induced in-plane tensile strain into the LCMO layers. However, different from the results found in this paper, the modulation amplitude of PR was approximately the same when PMN-PT was applied in positive or negative electric fields. Here, we can consider that the strain effect is dominant over the ferroelectric polarization effect. It was thought that both the strain effect and the ferroelectric polarization effect induced by ferroelectric poling always coexisted when the electric field was applied. However, the ferroelectric polarization effect only affects the PR when the film thickness is thin, because the accumulation or depletion of electrons only happens at the interface between film and substrate. When the film thickness is over a critical value, the ferroelectric polarization effect is rather limited, the decrease of resistance and modulation of PR is mainly due to the field induced strain effect.

In conclusion, we have investigated the possibility of electric control of photoinduced resistance changes for LSMO films grown on ferroelectric PMN-PT single crystals. The modulation of PR was strongly dependent on both the polarization state of the PMN-PT and the polarity of the electric field applied to the PMN-PT. This indicated that our results can be attributed to the coaction of the electric-field–induced polarization effect and the strain effect. This result is helpful not only for understanding the rich physics in manganites but also for their combination with developing novel functional devices.

* * *

We thank Prof. X. L. Li of the Shanghai Institute of Applied Physics, CAS for XRD measurements. This work has been supported by the Research Grant Council of Hong Kong (Project No. HKU702409P) and the URC of University of Hong Kong.

REFERENCES

[1] Helmholt R., Wecker J., Holzapfel B., Schultz L. and Samwer K., *Phys. Rev. Lett.*, **71** (1993) 2331.
[2] Takubo N., Ogimoto Y., Nakamura M., Tamaru H., Izumi M. and Miyano K., *Phys. Rev. Lett.*, **95** (2005) 017404.
[3] Matsuda K., Machida A., Moritomo Y. and Nakamura A., *Phys. Rev. B*, **58** (1998) R4203.
[4] Cui C. and Tyson T. A., *Phys. Rev. B*, **70** (2004) 094409.
[5] Zhao Y. G., Li J. J., Shreekala R., Drew H. D., Chen C. L., Cao W. L., Lee C. H., Rajeswari M., Ogale S. B., Ramesh R., Baskaran G. and Venkatesan T., *Phys. Rev. Lett.*, **81** (1998) 1310.
[6] Miyano K., Tanaka T., Tomioka Y. and Tokura Y., *Phys. Rev. Lett.*, **78** (1997) 4257.
[7] Huhtinen H., Laiho R. and Zakhvalinskii V., *Phys. Rev. B*, **71** (2005) 132404.
[8] Liu X. J., Moritomo Y., Nakamura A. and Asano H., *Jpn. J. Appl. Phys.*, **39** (2000) L1233.
[9] Jin K. X., Zhao S. G., Tan X. Y. and Chen C. L., *J. Phys. D: Appl. Phys.*, **41** (2008) 045105.
[10] Thiele C., Dörr K., Fähler S., Schultz L., Meyer D. C., Levin A. A. and Paufler P., *Appl. Phys. Lett.*, **87** (2005) 262502.
[11] Zheng R. K., Wang Y., Chan H. L. W., Choy C. L. and Luo H. S., *Appl. Phys. Lett.*, **90** (2007) 152904.
[12] Hong X., Posadas A. and Ahn C. H., *Appl. Phys. Lett.*, **86** (2005) 142501.
[13] Sheng Z. G., Gao J. and Sun Y. P., *Phys. Rev. B*, **79** (2009) 174437.
[14] Gao J. and Hu F. X., *Appl. Phys. Lett.*, **86** (2005) 092504.
[15] Guo E. J., Gao J. and Lu H. B., *Appl. Phys. Lett.*, **98** (2011) 081903.